

## Asymmetric nuclear matter: The role of the isovector scalar channel

B. Liu,<sup>1,2</sup> V. Greco,<sup>1</sup> V. Baran,<sup>1,3</sup> M. Colonna,<sup>1</sup> and M. Di Toro<sup>1</sup>

<sup>1</sup>Laboratorio Nazionale del Sud, Via S. Sofia 44, I-95123 Catania, Italy  
and University of Catania, I-95123 Catania, Italy

<sup>2</sup>Institute of High Energy Physics, Chinese Academy of Sciences, Beijing 100039, China

<sup>3</sup>NIPNE-HH, Bucharest, Romania

(Received 5 October 2001; published 19 March 2002)

We try to single out some qualitative effects of coupling to a  $\delta$ -isovector-scalar meson, introduced in a minimal way in a phenomenological hadronic field theory. Results for the equation of state (EOS) and the phase diagram of asymmetric nuclear matter (ANM) are discussed. We stress the consistency of the  $\delta$ -coupling introduction in a relativistic approach. Contributions to the slope and curvature of the symmetry energy and to the neutron-proton effective mass splitting appear particularly interesting. A more repulsive EOS for neutron matter at high baryon densities is expected. Effects on the critical properties of warm ANM, mixing mechanical and chemical instabilities and isospin distillation, are also presented. The  $\delta$  influence is mostly on the *isovectorlike* collective response. The results are largely analytical, and this makes the physical meaning quite transparent. Implications for nuclear structure properties of drip-line nuclei and for reaction dynamics with radioactive beams are finally pointed out.

DOI: 10.1103/PhysRevC.65.045201

PACS number(s): 21.65.+f, 21.30.Fe, 25.70.Pq, 24.10.Jv

### I. INTRODUCTION

Hadronic effective-field theories [quantum hadrodynamics (QHD)] represent a significant improvement in the understanding of static and dynamical properties of nuclear matter and finite nuclei, described as strongly interacting systems of baryons and mesons. The main application of this approach has been the relativistic mean-field (RMF) theory [1,2], extremely successful in nuclear structure studies [3–5].

In recent years, due to the possibilities opened by radioactive beam facilities, interest has moved toward a microscopic description of asymmetric nuclear systems, from the stability of drip-line nuclei to the phase diagram of asymmetric nuclear matter. The connection to astrophysics problems, supernova explosions, and neutron stars is also quite evident [6–9]. The isovector channel was introduced through a coupling to the charged vector  $\rho$  meson. In the Hartree approximation of the RMF approach, it leads to a simple linear increase of the symmetry term with the baryon density, without neutron or proton effective mass splitting [10]. A complete study of the corresponding phase diagram for asymmetric nuclear matter was performed in Ref. [11], with a thorough discussion of the new qualitative features of the liquid-gas phase transition.

In this work we focus our attention on the introduction of the coupling to the isovector scalar channel, through the exchange of a virtual charged  $\delta[a_0(980)]$  meson. In this way, as is well known in the isoscalar channel, we recover the genuine structure of the relativistic interactions, where one has a balance between scalar (attractive) and vector (repulsive) “potentials.” Actually the  $\delta$ -meson exchange is an essential ingredient of all nucleon-nucleon realistic potentials and its inclusion in the QHD scheme was already suggested [12], also on the basis of a relativistic Brueckner theory [13–15]. Some first results of structure calculations for exotic nuclei showed the importance of the  $\delta$  dynamics for the stability conditions of drip-line nuclei [15,16].

The aim of this paper is to present, within a RMF ap-

proach, the main expected effects of the  $\delta$  field on symmetry properties of the nuclear system, from the equation of state EOS to  $n,p$ -mass splitting, and in particular on the nuclear response in unstable regions. We recall that the study of symmetric and asymmetric nuclear matter properties under extreme conditions is of great relevance for understanding the nuclear interaction in the medium. In particular, a liquid-gas phase transition may occur in warm and dilute matter produced in heavy-ion collisions (multifragmentation events). This is one of the interesting open problems in theoretical and experimental nuclear physics. Isospin effects on heavy-ion collisions (fragmentation and collective flows) were widely discussed in recent years; see Refs. [17,18]. In this work we will try to offer a unified picture of the  $\delta$ -meson exchange influence on nuclear structure and dynamics.

In order to simplify the analysis and to pin down the most direct effects of the  $\delta$  contributions, we will follow a quite reduced version of the RMF approach, including all the isoscalar ( $\sigma, \omega$ ) and isovector ( $\delta, \rho$ ) fields. Nonlinear self-interaction terms are introduced only in the isoscalar scalar  $\sigma$  channel, essential in order to obtain the right incompressibility parameter at normal density  $\rho_0$  [19,20]. Such an approximation scheme of minimal self-interacting terms is actually physically well justified in the baryon density range of interest here, roughly up to  $2.5\rho_0$  [21]. Moreover, it is consistent with the RMF assumptions of neglecting retardation and finite range effects in the field dynamics [22]. We stress the presence of several points of interest in the isovector channel results in this baryon density region [24]:

(i) The slope of the symmetry term, the *symmetry pressure*, just below  $\rho_0$  is of relevant importance for nuclear structure, being directly linked to the thickness of the neutron skin in  $n$ -rich (stable and/or unstable) nuclei; see the recent discussions in Refs. [25–27]. Jointly to the  $n$ - $p$  effective masses, this is an essential ingredient for the stability of drip-line nuclei [15,16]. Dissipative reaction mechanisms with asymmetric ions also seem to be quite sensitive to the same quantity [28,29].

(ii) The nature of chemical instabilities and in general critical properties of warm and dilute asymmetric nuclear matter [11,30–33].

(iii) Isospin effects on the dynamics of heavy ion collisions at intermediate energies; see Ref. [18]. Reaction studies represent a very sensitive tool to test transport properties of symmetry effects,  $n$ - $p$  chemical potentials, and effective masses [34–36].

In this paper, we first determine the model parameters by fitting the properties of the symmetric and asymmetric nuclear matter at  $T=0$ . We then extend the investigation to finite temperature. In particular, we derive boundary regions for mechanical and chemical instabilities, and their dependence on the various mesons entering the theory.

This paper is organized as follows. In Sec. II, the equation of state for nuclear matter at a finite temperature is derived. Symmetry energies and effective masses are discussed in Sec. III, where the neutron matter EOS is also evaluated. The mechanical and chemical instabilities are studied in Sec. IV. General comments as well as a summary of the main conclusions are presented in Sec. V.

## II. EQUATION OF STATE FOR NUCLEAR MATTER AT FINITE TEMPERATURE

The starting point is the relativistic Lagrangian density of an interacting many-particle system consisting of nucleons, isoscalar (scalar  $\sigma$ , vector  $\omega$ ), and isovector (scalar  $\delta$ , vector  $\rho$ ) mesons:

$$\begin{aligned} \mathcal{L} = & \bar{\psi}[i\gamma_\mu\partial^\mu - (M_N - g_\sigma\phi - g_\delta\vec{\tau}\cdot\vec{\delta}) - g_\omega\gamma_\mu\omega^\mu \\ & - g_\rho\gamma^\mu\vec{\tau}\cdot\vec{b}_\mu]\psi + \frac{1}{2}(\partial_\mu\phi\partial^\mu\phi - m_\sigma^2\phi^2) - U(\phi) \\ & + \frac{1}{2}m_\omega^2\omega_\mu\omega^\mu + \frac{1}{2}m_\rho^2\vec{b}_\mu\cdot\vec{b}^\mu + \frac{1}{2}(\partial_\mu\vec{\delta}\cdot\partial^\mu\vec{\delta} - m_\delta^2\vec{\delta}^2) \\ & - \frac{1}{4}F_{\mu\nu}F^{\mu\nu} - \frac{1}{4}\vec{G}_{\mu\nu}\vec{G}^{\mu\nu}. \end{aligned} \quad (1)$$

Minimal self-interacting terms are included only in the  $\sigma$ -channel, as discussed in Sec. I.

Here  $\phi$  is the  $\sigma$ -meson field,  $\omega_\mu$  the  $\omega$ -meson field,  $\vec{b}_\mu$  the charged  $\rho$ -meson field, and  $\vec{\delta}$  the isovector scalar field of the  $\delta$ -meson. We define  $F_{\mu\nu} \equiv \partial_\mu\omega_\nu - \partial_\nu\omega_\mu$ ,  $\vec{G}_{\mu\nu} \equiv \partial_\mu\vec{b}_\nu - \partial_\nu\vec{b}_\mu$ .  $U(\phi)$  is the nonlinear potential of the  $\sigma$  meson:  $U(\phi) = \frac{1}{3}a\phi^3 + \frac{1}{4}b\phi^4$ .

The field equations in mean field approximation (RMF) are

$$\begin{aligned} [i\gamma_\mu\partial^\mu - (M_N - g_\sigma\phi - g_\delta\tau_3\delta_3) - g_\omega\gamma^0\omega_0 - g_\rho\gamma^0\tau_3b_0]\psi \\ = 0, \\ m_\sigma^2\phi + a\phi^2 + b\phi^3 = \bar{\psi}\psi = g_\sigma\rho_S, \\ m_\omega^2\omega_0 = g_\omega\bar{\psi}\gamma^0\psi = g_\omega\rho_B, \\ m_\rho^2b_0 = g_\rho\bar{\psi}\gamma^0\tau_3\psi = g_\rho\rho_{B3}, \\ m_\delta^2\delta_3 = g_\delta\bar{\psi}\tau_3\psi = g_\delta\rho_{S3}, \end{aligned} \quad (2)$$

where  $\rho_{B3} = \rho_{Bp} - \rho_{Bn}$  and  $\rho_{S3} = \rho_{Sp} - \rho_{Sn}$ ,  $\rho_B$  and  $\rho_S$  are the baryon and the scalar densities, respectively.

Neglecting the derivatives of mesons fields, in the mean-field approximation the energy-momentum tensor is given by

$$\begin{aligned} T_{\mu\nu} = & i\bar{\psi}\gamma_\mu\partial_\nu\psi + [\frac{1}{2}m_\sigma^2\phi^2 + U(\phi) + \frac{1}{2}m_\delta^2\vec{\delta}^2 - \frac{1}{2}m_\omega^2\omega_\lambda\omega^\lambda \\ & - \frac{1}{2}m_\rho^2\vec{b}_\lambda\vec{b}^\lambda]g_{\mu\nu}. \end{aligned} \quad (3)$$

The properties of nuclear matter at finite temperature are described by the thermodynamic potential  $\Omega$ . For a system in a volume  $V$  from statistical mechanics, we define  $\Omega = -pV = -(1/\beta)\ln Z$  [2], where  $\beta$  the inverse of temperature,  $\beta = 1/T$ , and  $Z$  is the grand partition function given by  $Z = \text{Tr}[e^{-\beta(\hat{H} - \sum_i \mu_i \hat{B}_i)}]$ . Here  $\hat{H}$  is the Hamiltonian operator, and  $\hat{B}_i$  and  $\mu_i$  are nucleon number operators and thermodynamic chemical potentials, respectively, ( $i = p, n$ ). The equation of state for nuclear matter at finite temperature can be obtained from the thermodynamic potential  $\Omega$ .

The energy density has the form

$$\begin{aligned} \epsilon = & \sum_{i=n,p} 2 \int \frac{d^3k}{(2\pi)^3} E_i^*(k)[n_i(k) + \bar{n}_i(k)] + \frac{1}{2}m_\sigma^2\phi^2 + U(\phi) \\ & + \frac{1}{2}m_\omega^2\omega_0^2 + \frac{1}{2}m_\rho^2b_0^2 + \frac{1}{2}m_\delta^2\delta_3^2, \end{aligned} \quad (4)$$

and the pressure is

$$\begin{aligned} P = & \sum_{i=n,p} \frac{2}{3} \int \frac{d^3k}{(2\pi)^3} \frac{k^2}{E_i^*(k)} [n_i(k) + \bar{n}_i(k)] - \frac{1}{2}m_\sigma^2\phi^2 \\ & - U(\phi) + \frac{1}{2}m_\omega^2\omega_0^2 + \frac{1}{2}m_\rho^2b_0^2 - \frac{1}{2}m_\delta^2\delta_3^2, \end{aligned} \quad (5)$$

where  $E_i^* = \sqrt{k^2 + M_i^{*2}}$ . The nucleon effective masses are defined as

$$M_i^* = M_N - g_\sigma\phi \mp g_\delta\delta_3 \quad (-\text{proton}, +\text{neutron}). \quad (6)$$

$n_i(k)$  and  $\bar{n}_i(k)$  in Eqs. (4) and (5) are the fermion and antifermion distribution functions for protons ( $i = p$ ) and neutrons ( $i = n$ ):

$$n_i(k) = \frac{1}{1 + \exp\{(E_i^*(k) - \mu_i^*)/T\}} \quad (7)$$

and

$$\bar{n}_i(k) = \frac{1}{1 + \exp\{(E_i^*(k) + \mu_i^*)/T\}}. \quad (8)$$

The effective chemical potentials  $\mu_i^*$  are given in terms of the vector meson mean fields

$$\mu_i = \mu_i^* - g_\omega\omega_0 \mp g_\rho b_0 \quad (-\text{proton}, +\text{neutron}), \quad (9)$$

where  $\mu_i$  are the thermodynamical chemical potentials  $\mu_i = \partial\epsilon/\partial\rho_i$ . At zero temperature they reduce to the Fermi energies  $E_{Fi} \equiv \sqrt{k_{Fi}^2 + M_i^{*2}}$ .

The same results can be directly obtained from the expectation value of the energy-momentum tensor, showing the thermodynamical consistency of the mean-field approximation [2].

By using the field equations for mesons, the equations of state for thermal matter can be rewritten as

$$\epsilon = \sum_{i=n,p} 2 \int \frac{d^3k}{(2\pi)^3} E_i^*(k) [n_i(k) + \bar{n}_i(k)] + \frac{1}{2} m_\sigma^2 \phi^2 + U(\phi) + \frac{g_\omega^2}{2m_\omega^2} \rho_B^2 + \frac{g_\rho^2}{2m_\rho^2} \rho_{B3}^2 + \frac{g_\delta^2}{2m_\delta^2} \rho_{S3}^2 \quad (10)$$

and

$$P = \sum_{i=n,p} \frac{2}{3} \int \frac{d^3k}{(2\pi)^3} \frac{k^2}{E_i^*(k)} [n_i(k) + \bar{n}_i(k)] - \frac{1}{2} m_\sigma^2 \phi^2 - U(\phi) + \frac{g_\omega^2}{2m_\omega^2} \rho_B^2 + \frac{g_\rho^2}{2m_\rho^2} \rho_{B3}^2 - \frac{g_\delta^2}{2m_\delta^2} \rho_{S3}^2. \quad (11)$$

We recall that the baryon densities  $\rho_B$  are given by ( $\gamma$  is the spin or isospin multiplicity)

$$\rho_B = \gamma \int \frac{d^3k}{(2\pi)^3} [n(k) - \bar{n}(k)], \quad (12)$$

while the scalar densities  $\rho_S$  are

$$\rho_S = \gamma \int \frac{d^3k}{(2\pi)^3} \frac{M^*}{E^*} [n(k) + \bar{n}(k)]. \quad (13)$$

At the temperatures of interest here the antibaryon contributions are actually negligible.

In order to study the asymmetric nuclear matter, we introduce an asymmetry parameter  $\alpha$  defined as  $\alpha = (\rho_{Bn} - \rho_{Bp})/\rho_B = (N - Z)/A$ . The energy density and pressure for symmetric and asymmetric nuclear matter and the  $n, p$  effective masses can be self-consistently calculated from Eqs. (6)–(13), just in terms of the four boson coupling constants,  $f_i \equiv (g_i^2/m_i^2)$ ,  $i = \sigma, \omega, \rho, \delta$ , and the two parameters of the  $\sigma$  self-interacting terms:  $A \equiv a/g_\sigma^3$  and  $B \equiv b/g_\sigma^4$ .

The isoscalar meson parameters are fixed from symmetric nuclear matter properties at  $T=0$ : saturation density  $\rho_0 = 0.16 \text{ fm}^{-3}$ , binding energy  $E/A = -16 \text{ MeV}$ , nucleon effective mass  $M^* = 0.75M_N$  ( $M_N = 939 \text{ MeV}$ ), and incompressibility  $K_V = 240 \text{ MeV}$  at  $\rho_0$ . The fitted  $f_\sigma, f_\omega, A$ , and  $B$  parameters are reported in Table I. They have quite standard values for these minimal nonlinear RMF models.

In Table I we also report the NL3 parametrization, widely used in nuclear structure calculations [4]. We recall that the NL3 saturation properties for symmetric matter are chosen as  $\rho_0 = 0.148 \text{ fm}^{-3}$ ,  $M^* = 0.6M_N$ , and  $K_V = 271.8 \text{ MeV}$ . The symmetry parameter (see Sec. III) is  $a_4 = 37.4 \text{ MeV}$ .

The phase diagram (pressure isotherms) obtained with our set I is shown in Fig. 1. The local minimum disappears at the critical temperature  $T_c$ , determined by  $(\partial P/\partial \rho)|_{T_c}$

TABLE I. Parameter sets.

Parameter	Set I	Set II	NL3
$f_\sigma$ (fm <sup>2</sup> )	10.33	same	15.73
$f_\omega$ (fm <sup>2</sup> )	5.42	same	10.53
$f_\rho$ (fm <sup>2</sup> )	0.95	3.15	1.34
$f_\delta$ (fm <sup>2</sup> )	0.00	2.50	0.00
$A$ (fm <sup>-1</sup> )	0.033	same	-0.01
$B$	-0.0048	same	-0.003

$= (\partial^2 P/\partial \rho^2)|_{T_c} = 0$ . The obtained critical temperature of symmetric matter is  $T_c = 15.86 \text{ MeV}$ .

### III. SYMMETRY ENERGY

Symmetry properties of asymmetric nuclear matter are univocally fixed from the coupling constants of the isovector channels [37]. Experimentally we have just one relatively well-known quantity, the bulk symmetry energy  $a_4$  of the Weizsaecker mass formula, in the range 30–35 MeV. In all RMF models with only the isovector  $\rho$  meson, this assigns the  $f_\rho$  constant, that also gives the “slope” of the symmetry term (the *symmetry pressure*) [10], apart from small nonlinear contributions [23].

When we further include the  $\delta$  meson, from the  $a_4$  value we will now fix only a combination of the two coupling constants. Meanwhile,  $\delta$  itself will imply interesting contributions to the slope and curvature of the symmetry energy and a neutron-proton effective mass splitting. These will be the main points discussed in the following. We note that most results are analytical, and this will largely improve the physical understanding of the effects due to the coupling to the  $\delta$  isovector scalar channel. The symmetry energy in asymmetric NM is defined from the expansion of the energy per nucleon  $E(\rho_B, \alpha)$  in terms of the asymmetry parameter

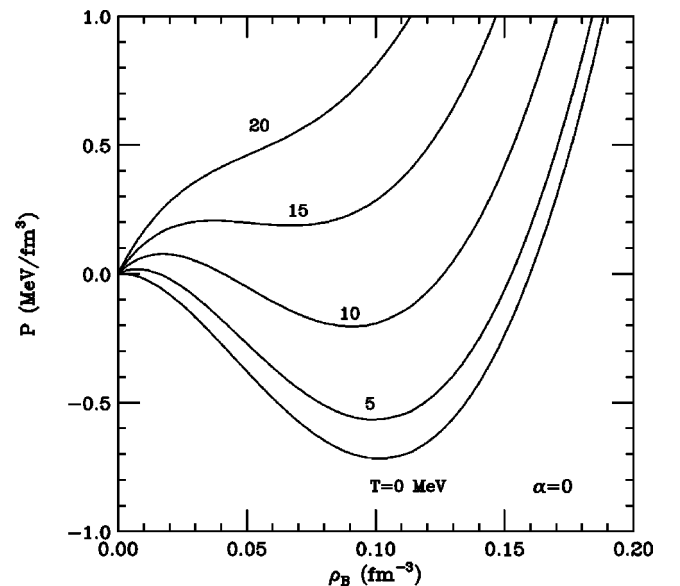


FIG. 1. Pressure as a function of the baryon density for symmetric nuclear matter ( $\alpha=0$ ) at different temperatures.

$$E(\rho_B, \alpha) \equiv \frac{\epsilon(\rho_B, \alpha)}{\rho_B} = E(\rho_B) + E_{sym}(\rho_B)\alpha^2 + O(\alpha^4) + \dots, \quad (14)$$

and so, in general,

$$E_{sym} \equiv \frac{1}{2} \left. \frac{\partial^2 E(\rho_B, \alpha)}{\partial \alpha^2} \right|_{\alpha=0} = \frac{1}{2} \rho_B \left. \frac{\partial^2 \epsilon}{\partial \rho_{B3}^2} \right|_{\rho_{B3}=0} \quad (15)$$

### Bulk symmetry parameter

The bulk symmetry parameter  $a_4$  is just the value of  $E_{sym}$  corresponding to the normal density  $\rho_B = \rho_0$ , at  $T=0$ . We first discuss the case at zero temperature, in order to fix the isovector coupling constants. From Eqs. (10) and (15) we can easily obtain an explicit expression for the symmetry energy [12]

$$E_{sym}(\rho_B) = \frac{1}{6} \frac{k_F^2}{E_F} + \frac{1}{2} f_\rho \rho_B - \frac{1}{2} f_\delta \frac{M^{*2} \rho_B}{E_F^2 [1 + f_\delta A(k_F, M^*)]}, \quad (16)$$

where  $k_F$  is the nucleon Fermi momentum corresponding to  $\rho_B$ ,  $E_F \equiv \sqrt{(k_F^2 + M^{*2})}$ , and  $M^*$  is the effective nucleon mass in symmetric NM,  $M^* = M_N - g_\sigma \phi$ .

The integral

$$A(k_F, M^*) \equiv \frac{4}{(2\pi)^3} \int d^3k \frac{k^2}{(k^2 + M^{*2})^{3/2}} \quad (17)$$

has a simple analytical structure which makes the effect of the  $\delta$  meson on the symmetry energy quite transparent. With some algebra we can obtain

$$A(k_F, M^*) = 3 \left( \frac{\rho_S}{M^*} - \frac{\rho_B}{E_F} \right), \quad (18)$$

making use of

$$\rho_S(T=0) = \frac{M^*}{\pi^2} \left[ k_F E_F - M^{*2} \ln \left( \frac{k_F + E_F}{M^*} \right) \right],$$

$$\rho_B(T=0) = \frac{2}{3\pi^2} k_F^3. \quad (19)$$

Expanding the scalar density in terms of  $(k_F/M^*)^2$  [2], Eq. (18) can be written as

$$A(k_F, M^*) = \frac{3\rho_B}{M^*} \left[ \frac{1}{5} \left( \frac{k_F}{M^*} \right)^2 - \frac{3}{14} \left( \frac{k_F}{M^*} \right)^4 - \frac{5}{24} \left( \frac{k_F}{M^*} \right)^6 + \dots \right],$$

that can be used to derive a similar expansion for the symmetry energy [Eq. (16)].

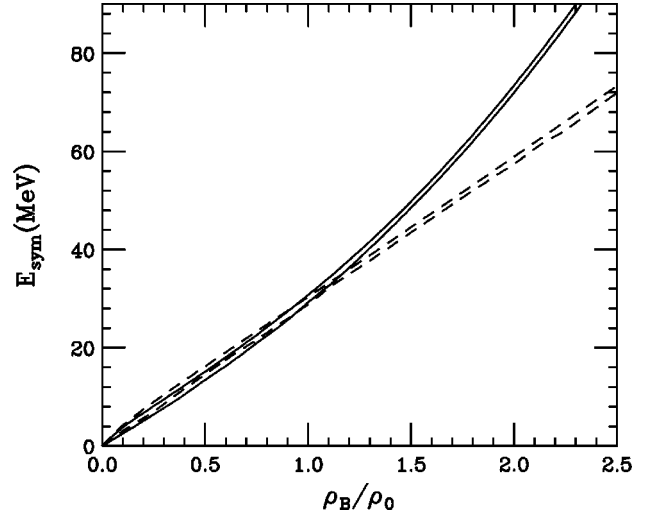


FIG. 2. Total (kinetic + potential) symmetry energy as a function of the baryon density. Dashed lines:  $(\rho)$ . Solid lines:  $(\rho + \delta)$ . Upper curves: zero temperature. Lower curves:  $T = 8$  MeV.

We see that  $A(k_F, M^*)$  is certainly very small at low densities, below  $\rho_0$ . It can still be neglected up to a baryon density  $\rho_B \approx 3\rho_0$ , where it reaches the value  $0.045 \text{ fm}^{-2}$  (with our symmetric NM parameters), i.e., a correction of about 10% in the denominator of Eq. (16).

Then in the density range of interest here we can use, at leading order, a much simpler form of the symmetry energy, with transparent  $\delta$ -meson effects:

$$E_{sym}(\rho_B) = \frac{1}{6} \frac{k_F^2}{E_F} + \frac{1}{2} \left[ f_\rho - f_\delta \left( \frac{M^*}{E_F} \right)^2 \right] \rho_B. \quad (20)$$

We see that, when  $\delta$  is included, the observed  $a_4$  value actually assigns the combination  $[f_\rho - f_\delta (M^*/E_F)^2]$  of the  $(\rho, \delta)$  coupling constants. If  $f_\delta \neq 0$  we have to increase the  $\rho$  coupling (see Fig. 1 of Ref. [12]). In our calculations we use the value  $a_4 = 30.5 \text{ MeV}$ . In Table I set I corresponds to  $f_\delta = 0$ . In set II  $f_\delta$  is chosen as  $2.5 \text{ fm}^2$ . Although this value is relatively well justified [39], we stress that aim of this work is just to show the main qualitative effects of the  $\delta$  coupling.

In order to have the same  $a_4$ , we must increase the  $\rho$ -coupling constant of a factor of 3, up to  $f_\rho = 3.15 \text{ fm}^2$ . From the structure of Eqs. (16) and (20), it is clear that there is a connection between the scalar field (isoscalar  $\sigma$  and isovector  $\delta$ ) contributions, since both are acting on effective masses. A strong  $\sigma$  coupling (smaller  $M^*$ , e.g., see the NL3 parametrization) can compensate for a strong  $\delta$  coupling. In our evaluation we keep the  $\sigma$  parameters ( $f_\sigma, A, B$ ) fixed, leading to  $M^* = 0.75M_N$ . In any case a larger value of  $E_{sym}$  at high baryon densities, due to the relativistic mechanism discussed in the following (see Fig. 2), will be always present when  $\delta$  is included.

At subnuclear densities,  $\rho_B < \rho_0$ , in both cases  $(\rho)$  and  $(\rho + \delta)$ , from Eq. (20) we have an almost linear dependence of  $E_{sym}$  on the baryon density, since  $M^* \approx E_F$  as a good

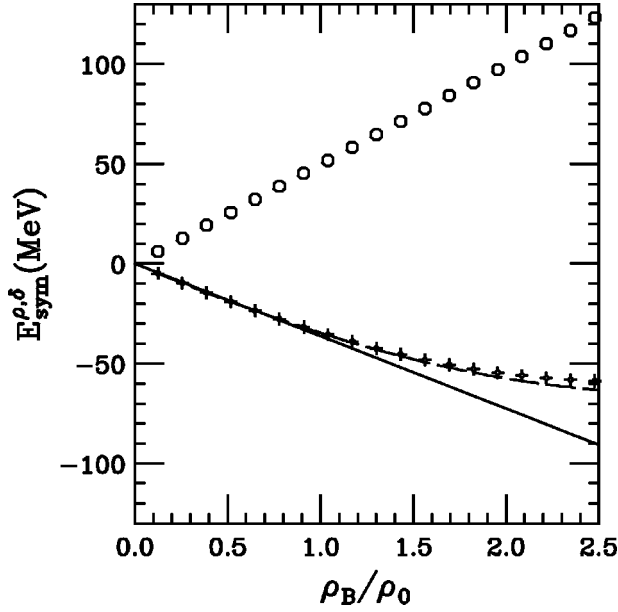


FIG. 3.  $\rho$  (open circles) and  $\delta$  (crosses) contributions to the symmetry energy, and the second and third terms of Eq. (16). The dashed line is the approximate  $\delta$  contribution of Eq. (20), see the text. The solid line is a linear extrapolation of the low-density behavior, plotted to guide the eye.

approximation. Around and above  $\rho_0$ , we expect a steeper increase in the  $(\rho + \delta)$  case since  $M^*/E_F$  is decreasing; see Fig. 2.

This is an interesting aspect to look at in more detail since it actually represents a general relativistic effect due to the coupling to scalar mesons. In some sense it is the equivalent, in the isovector channel ( $\delta$  vs  $\rho$ ) (i.e. for the symmetry energy), of the saturation mechanism we have in the isoscalar channel ( $\sigma$  vs  $\omega$ ) for the symmetric matter.

The scalar charged  $\delta$  meson, like the neutral  $\sigma$  meson, acts on the nucleon effective masses, introducing an  $n$ - $p$  splitting; see Eq. (6). This causes a negative contribution to  $E_{sym}$ , [Eqs. (16) and (21)], since it reduces the gap between  $n$ - $p$  Fermi energies, due to the different Fermi momenta in asymmetric NM. In fact, in  $n$ -rich matter the neutron Fermi momentum increases while the neutron effective mass decreases see [Eq. (6) and Fig. 6] (the opposite occurs for protons). Such a negative  $\delta$  contribution is reduced at high densities due to the ‘‘Lorentz contraction’’ factor  $(M^*/E_F)^2$  [Eqs. (16) and (20)], that in general gives the attenuation of the scalar interactions with increasing baryon density.

We stress the consistent picture of a symmetry energy built from the balance of scalar (attractive) and vector (repulsive) contributions, with the scalar channel becoming weaker with increasing baryon density. This is indeed the isovector counterpart of the saturation mechanism occurring in the isoscalar channel for the symmetric nuclear matter. From such a scheme we obtain a further strong fundamental support for the introduction of the  $\delta$  coupling in the symmetry energy evaluation.

In Fig. 3, using our parametrizations, we quantitatively show the interplay of the two contributions ( $\rho$  and  $\delta$ ) to  $E_{sym}$  [the second and third terms of Eqs. (16) and (20)], as a

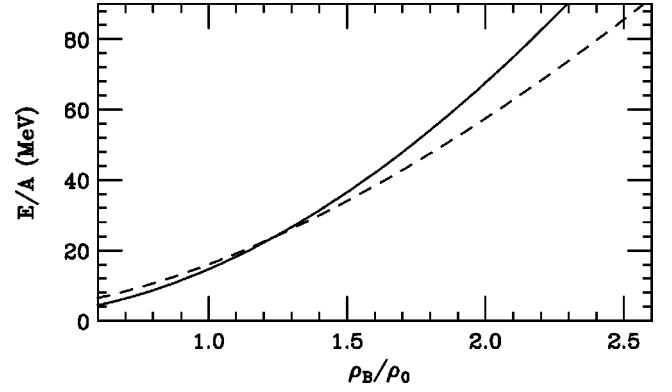


FIG. 4. EOS for pure neutron matter. Dashed line: ( $\rho$ ). Solid line: ( $\rho + \delta$ ).

function of the baryon density. The crosses (negative  $\delta$  contribution) follow a linear behavior up to roughly  $\rho_0$ , and then tend to saturate due to the Lorentz contraction factor. Correspondingly, we see the increase of the total  $E_{sym}$  shown in Fig. 2. We note the accuracy of the approximate  $\delta$  contribution given by Eq. (20) (dashed line in Fig. 3).

In Fig. 4 we show the equation of state (energy per nucleon) for pure neutron matter ( $\alpha=1$ ) obtained with the two parameter sets, I ( $\rho$ ) and II ( $\rho + \delta$ ) [40]. The values are in good agreement with recent nonrelativistic quantum Monte Carlo variational calculations with realistic two- and three-body forces [41]. The inclusion of the  $\delta$  coupling leads to a larger repulsion at baryon densities roughly above  $1.5\rho_0$ . This could be of interest for the structure of neutron stars and the possibility of a transition to different forms of nuclear matter.

From the previous analysis also we expect to see interesting  $\delta$  effects on the slope (symmetry pressure) and curvature (symmetry incompressibility) of the symmetry energy around  $\rho_0$ , of relevant physical meaning. This will be the main subject of the following discussion.

#### Symmetry pressure and symmetry incompressibility

In order to have a quantitative evaluation of the  $\delta$  effects, we use the expansion of the symmetry energy around  $\rho_0$  [42,43],

$$E_{sym}(\rho_B) = a_4 + \frac{L}{3} \left( \frac{\rho_B - \rho_0}{\rho_0} \right) + \frac{K_{sym}}{18} \left( \frac{\rho_B - \rho_0}{\rho_0} \right)^2 + \dots, \quad (21)$$

with  $L$  and  $K_{sym}$ , respectively, related to slope and curvature of the symmetry energy at  $\rho_0$

$$L = 3\rho_0 \left( \frac{\partial E_{sym}}{\partial \rho_B} \right) \Big|_{\rho_B = \rho_0}$$

and

$$K_{sym} = 9\rho_0^2 \left( \frac{\partial^2 E_{sym}}{\partial \rho_B^2} \right) \Big|_{\rho_B = \rho_0}. \quad (22)$$

From Eq. (20) we obtain a potential contribution to the density variation of  $E_{sym}$  given by (after some algebra)

$$\left. \frac{\partial E_{sym}}{\partial \rho_B} \right|_{pot} = \frac{1}{2} \left[ f_\rho - f_\delta \left( \frac{M^*}{E_F} \right)^2 \right] + f_\delta \left( \frac{M^* k_F}{E_F^2} \right)^2 \left[ \frac{1}{3} - \frac{\rho_B}{M^*} \frac{\partial M^*}{\partial \rho_B} \right]. \quad (23)$$

Around normal density  $\rho_0$  the first term is fixed by the  $a_4$  value [cf. Eq. (20)]. The second term [always positive since  $(\partial M^*/\partial \rho_B) < 0$ ] gives a net increase of the slope, due to the  $\delta$  introduction.

To be more quantitative, with our parametrization we obtain a potential contribution to  $L$  of 45 MeV from the first term and a genuine  $\delta$  extra contribution of about 20 MeV from the second one. When we include also the kinetic part [from the first term of Eq. (20)] we have a total slope parameter going from  $L(\rho) = +84$  MeV to  $L(\rho + \delta) = +103$  MeV.

We note again that the slope parameter, or equivalently the symmetry pressure  $P_{sym} \equiv \rho_0 L/3$ , is of great importance for structure properties, being linked to the thickness of the neutron skin in  $n$ -rich (stable and/or unstable) nuclei [24–27], and to the assessment of the drip line [16]. Moreover the same parameter gives an estimate of the shift of the saturation density with asymmetry (at the lowest order in  $\alpha^2$ ),

$$\Delta \rho_0(\alpha) = - \frac{3\rho_0 L}{K_V(\alpha=0)} \alpha^2, \quad (24)$$

that can be easily obtained from a linear expansion around the symmetric value  $\rho_0(\alpha=0)$  [29].

Equation (24) has a simple physical meaning: in order to compensate for the symmetry pressure in asymmetric matter, we have to move the zero of the  $P(\rho_B)$  curve to lower densities. The amount of the shift will be inversely proportional to the slope, given by the incompressibility. All this can be seen in Fig. 5, where we report the total pressure  $P(\rho_B)$  for various asymmetries, at zero temperature, in the two cases,  $\rho$  meson only (dashed lines) and  $(\rho + \delta)$  (solid lines). It is instructive to perform a similar discussion for the curvature parameter  $K_{sym}$  [Eq. (21)]. Now the potential contribution is *exclusively* given by the  $\delta$  meson, with a definite positive sign, as we can see from the previous discussion. This will have a large effect on the total, since the kinetic part is quite small [45]. If we compare with nonrelativistic effective parametrizations [44,43], when we add the  $\delta$  meson we move from a linear to a roughly parabolic  $\rho_B$  dependence of the symmetry energy.

With our parameters we pass from a  $K_{sym}(\rho) = +7$  MeV (only kinetic) to a  $K_{sym}(\rho + \delta) = +120$  MeV. This quantity appears extremely interesting to look at experimentally, as recently suggested from reaction measurements [43]. The problem is that the effect on the total incompressibility of asymmetric matter, that likely could be easier to

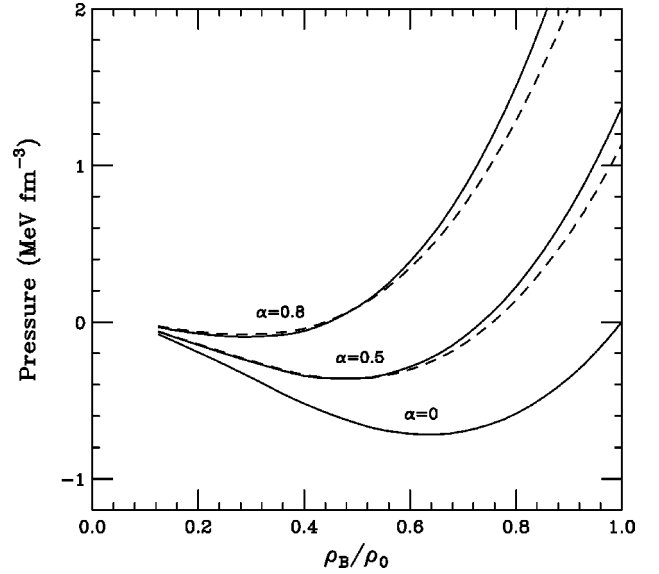


FIG. 5. Pressure as a function of the baryon density at zero temperature for various asymmetries  $\alpha = 0$  (bottom), 0.5 (middle), and 0.8 (top). Dashed lines:  $(\rho)$ . Solid lines:  $(\rho + \delta)$ .

measure, is not trivial. We can evaluate a shift of the incompressibility with asymmetry, at the same  $\alpha^2$  order as in Eq. (24), as [42,29]

$$\Delta K_V(\alpha) = (K_{sym} - 6L) \alpha^2. \quad (25)$$

What really matters for the total incompressibility is the combination  $(K_{sym} - 6L)$ , with the possibility of a compensation between the two terms. Just by chance this is actually what happens in our calculations, since, for the above combination, we obtain  $-497$  MeV in the case of only  $\rho$  coupling, and  $-504$  MeV when we also add the  $\delta$ . Indeed, from Fig. 5 that we see the slopes of the pressure around equilibrium density [ $P(\rho_0) = 0$ ] are very close in the two cases:  $(\rho)$  and  $(\rho + \delta)$ .

### Effective-mass splitting

Another interesting result of the  $\delta$ -meson coupling is the  $n, p$  effective-mass splitting in asymmetric matter [12]; see Eq. (6). In Fig. 6 we report the baryon density dependence of the  $n, p$  effective masses for  $\alpha = 0.5$  ( $N = 3Z$ ) asymmetry, calculated with our set II parameters, compared to the symmetric case [46].

We obtain a splitting of the order of 15% at normal density  $\rho_0$ , increasing with baryon density. Unfortunately from the present nuclear data we gain only as light knowledge of this effect, due to the low asymmetries available. This issue will be quite relevant in the study of drip-line nuclei. Moreover, we can expect important effects on transport properties (fast particle emission, collective flows) of the dense and asymmetric NM that will be reached in radioactive beam collisions at intermediate energies.

The sign itself of the splitting would be very instructive. As we can see from Eq. (6) in  $n$ -rich systems we expect a neutron effective mass always smaller than the proton effective

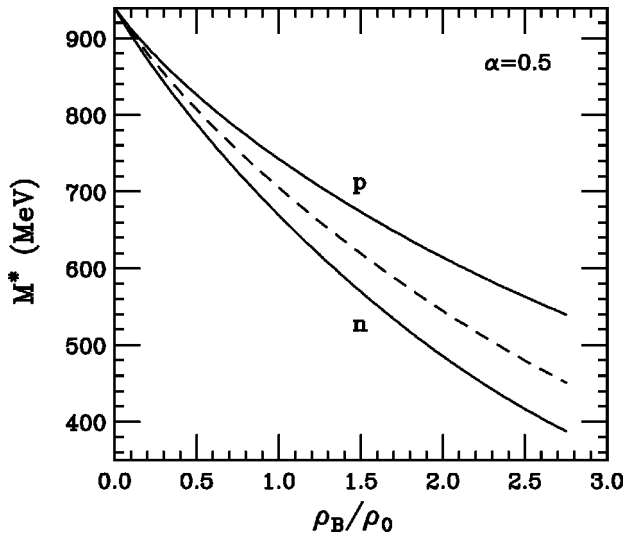


FIG. 6. Neutron and proton effective masses vs the baryon density for  $\alpha=0.5$  ( $N=3Z$ ). The dashed line corresponds to symmetric nuclear matter.

tive mass. The same is predicted from more microscopic relativistic Dirac-Brueckner calculations [15]. At variance, nonrelativistic Brueckner-Hartree-Fock calculations lead to the opposite conclusions [9,47]. Still, in the nonrelativistic picture quite contradictory results are obtained with Skyrme effective forces. The most recent parametrizations, SLy type [48], of Skyrme forces give a proton effective mass above the neutron one, in agreement with our calculations. Previous Skyrme-like forces, instead, yield a splitting in the opposite direction, but also show unpleasant behaviors in the spin channel (collapse of polarized neutron matter; see the discussion in Ref. [48]). We note again that, as discussed above, a decreasing neutron effective mass in  $n$ -rich matter is behind the relativistic mechanism for the symmetry energy, i.e., the balance of scalar (attractive) and vector (repulsive) contributions in the isovector channel.

#### Finite-temperature effects

In the temperature range of interest in this paper, below the critical temperature  $T_c$  of the liquid-gas phase transition, of the order of 15–16 MeV (see Fig. 1), temperature effects on the symmetry properties are not expected to be large. Indeed the contributions of antifermions, that could modify all the terms with the scalar densities [see Eq. (13)], are still very reduced. In Fig. 2 we also present the symmetry energies calculated at  $T=8$  MeV (lower solid and dashed curves). For both cases,  $\rho$  and  $(\rho + \delta)$ , the variation is quite small. We have a reduction mainly coming from the kinetic contribution due to the smoothing of the  $n, p$  Fermi distributions. We note that this result is in full agreement with relativistic Brueckner-Hartree-Fock calculations [49].

The effect for the mass splitting, given by a difference of scalar densities, is even smaller. In Sec. IV, we will study in detail the phase diagram of heated asymmetric nuclear matter, focusing in particular on the instability regions.

#### IV. MECHANICAL AND CHEMICAL INSTABILITIES

Heavy-ion collisions can provide the possibility to study equilibrated nuclear matter far away from normal conditions, i.e., to sample regions of the NM phase diagram. In particular the process of multifragmentation allows one to probe dilute nuclear matter at finite temperatures. In the symmetric case (see Fig. 1), we expect to see a phase transition of first order of liquid-gas type, as suggested from the very first equations of state built from effective interactions [50–52].

The multifragmentation phenomenon may be interpreted as a signal of such a phase transition in a finite system, when the nuclear matter in the expansion phase enters the region of spinodal (mechanical) instability. However, nuclear matter is a two-component system consisting of neutrons and protons: binary systems have more complicated phase diagrams due to their concentration degrees of freedom. In particular, for asymmetric nuclear matter an interesting feature in the liquid-gas phase transition is expected; the onset of a coupling to chemical instabilities (component separation). This will show up in the nature of the unstable modes, the mixture of density and charge fluctuations leading to an isospin distillation effect [11,30,33]. Indeed, equilibrium thermodynamics as well as nonequilibrium kinetics both predict that an asymmetric system will separate into more symmetric larger fragments (a “liquid” phase) and into neutron-rich light fragments (a “gas” phase). So the chemical instability can be investigated experimentally just by measuring the  $N/Z$  ratio, or isospin content, of the fragments.

Since the effect is driven by the isospin-dependent part of the nuclear equation of state, here we will look at the influence of the  $\delta$  coupling on this new liquid-gas phase transition. It is known that the stability condition of a two-component,  $n$ - $p$ , thermodynamical system is given by

$$\left(\frac{\partial P}{\partial \rho}\right)_{T,y} \left(\frac{\partial \mu_p}{\partial y}\right)_{T,P} > 0, \quad (26)$$

where  $P$  is the pressure,  $\mu_p$  is the proton chemical potential, and  $y$  the proton fraction  $Z/A$ , related to the asymmetry parameter  $\alpha = 1 - 2y$ .

Equation (26) is equivalent to set the free energy to be a convex function in the space of the  $n, p$  density oscillations:  $\delta\rho_n$  and  $\delta\rho_p$ . In charge symmetric matter, *isoscalar* (total density)  $\delta\rho_n + \delta\rho_p$  and *isovector* (concentration)  $\delta\rho_n - \delta\rho_p$  oscillations are not coupled, and we have two separate conditions for instability

$$\left(\frac{\partial P}{\partial \rho}\right)_{T,y} \leq 0; \quad (27)$$

*mechanical*, i.e. vs density oscillations (the spinodal region); and

$$\left(\frac{\partial \mu_p}{\partial y}\right)_{T,P} \leq 0, \quad (28)$$

*chemical*, i.e., vs concentration oscillations.

In asymmetric matter the isoscalar and isovector modes are coupled, and the two separate inequalities no longer maintain a physical meaning, in the sense that they do not select the nature of the instability. Inside the general condition [Eq. (26)] the corresponding unstable modes are a mixing of density and concentration oscillations, very sensitive to the charge dependent part of the nuclear interaction in the various instability regions [33].

In dilute asymmetric NM ( $n$ -rich), the normal unstable modes for all realistic effective interactions are still *isoscalarlike*, i.e., in-phase  $n$ - $p$  oscillations but with a larger proton component [33]. This leads to a more symmetric high-density (liquid) phase everywhere under the instability line defined by Eq. (26), and consequently to a more neutron-rich gas (*isospin distillation*). Such a “chemical effect” is driven by the increasing symmetry repulsion going from low density to roughly saturation value, and so it appears quite sensitive to the symmetry energy of the effective interaction used at subnuclear densities. It could provide a good opportunity to differentiate the various EOS isospin dependences [53].

In this section we study the effect of the  $\delta$  coupling on the instability region given by Eq. (26) in dilute asymmetric nuclear matter, and on the structure of the corresponding unstable modes. We start from an identity valid for any binary thermodynamical system

$$\begin{aligned} & \left( \frac{\partial \mu_p}{\partial \rho_p} \right)_{T, \rho_n} \left( \frac{\partial \mu_n}{\partial \rho_n} \right)_{T, \rho_p} - \left( \frac{\partial \mu_p}{\partial \rho_n} \right)_{T, \rho_p} \left( \frac{\partial \mu_n}{\partial \rho_p} \right)_{T, \rho_n} \\ &= \frac{1}{(1-y)\rho^2} \left( \frac{\partial P}{\partial \rho} \right)_{T, y} \left( \frac{\partial \mu_p}{\partial y} \right)_{T, P}, \end{aligned} \quad (29)$$

where  $\mu_q$ ,  $\rho_q$  ( $q=n, p$ ) are respectively neutron or proton chemical potentials and densities. From our knowledge of the chemical potential on each isotherm [Eq. (9)], we can easily compute the limits of the instability region in the  $T, \rho_B$  plane for dilute asymmetric NM in the two choices, without and with the  $\delta$  meson.

The results are reported in Fig. 7. The  $\delta$  inclusion (solid lines) does not appear affect the instability limits much, even at relatively large asymmetry  $\alpha=0.8$  ( $N \sim 9Z$ ). We note a small reduction and a shift to the left (lower densities) of the whole region: this can be understood in terms of the larger symmetry repulsion, see Fig. 3.

We can understand the relatively small  $\delta$  effect on the stability border by remembering that, for low densities, well below  $\rho_0$ , the symmetry term has roughly the same linear behavior in both  $(\rho)$  and  $(\rho + \delta)$  schemes, fixed by the  $a_4$  parameter [see the discussion after Eq. (20)]. Only for very large asymmetries does it appears relatively easier for the  $\delta$  case to be in the stable liquid phase.

A rather larger difference can be seen in the behavior of the quantity [Eq. (26)] inside the instability region. This is plotted in Fig. 8 for various asymmetries at zero temperature, and in Fig. 9 at various temperatures for a fixed asymmetry

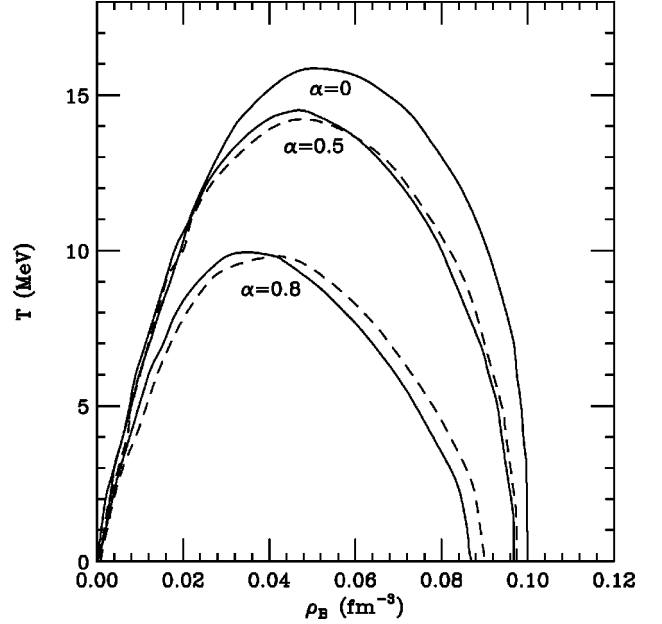


FIG. 7. Limits of the instability region in the  $T, \rho_B$  plane for various asymmetries. Dashed lines:  $(\rho)$ . Solid lines:  $(\rho + \delta)$  [for  $\alpha \neq 0$ ].

$\alpha=0.5$  ( $N=3Z$ ). The solid curves (with  $\delta$  coupling) are systematically above the dashed ones, a signature of a weaker instability.

In order to better understand the origin of such effect, we also study the structure of the corresponding unstable modes. We follow the Landau dispersion relation approach to small-amplitude oscillations in Fermi liquids [54,55,31,32]. For two-component  $(n, p)$  matter the interaction is characterized by the Landau parameters  $F_0^{q, q'}, (q, q') = (n, p)$ , defined as

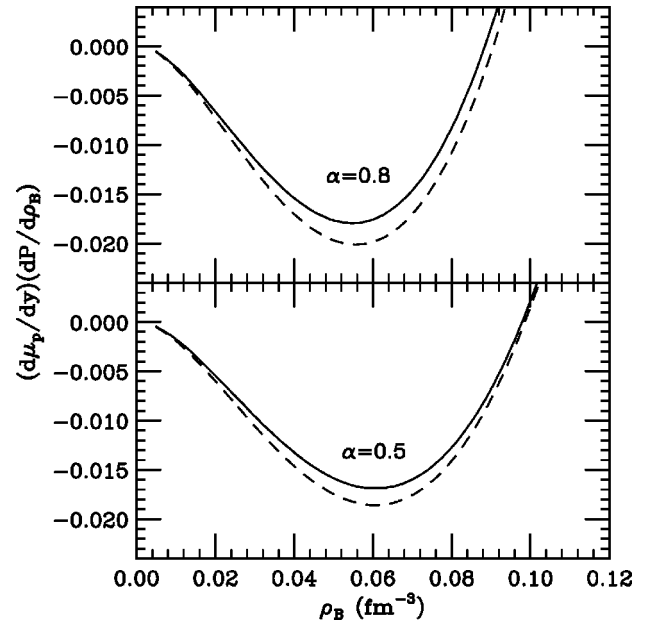


FIG. 8. The quantity [Eq. (26)] inside the instability region at  $T=0$  and various asymmetries. Dashed lines:  $(\rho)$ . Solid lines:  $(\rho + \delta)$ .

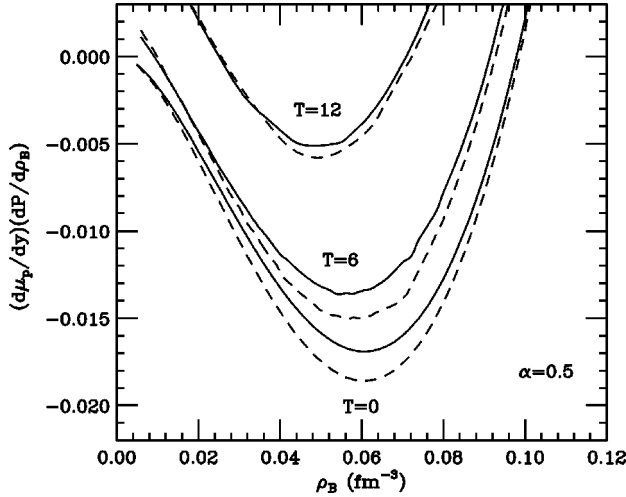


FIG. 9. The same as in Fig. 8 at various temperatures and fixed asymmetry  $\alpha=0.5$ . Dashed lines:  $(\rho)$ . Solid lines:  $(\rho + \delta)$ .

$$N_q(T) \frac{\partial \mu_q}{\partial \rho_{q'}} \equiv \delta_{q,q'} + F_0^{q,q'}, \quad (30)$$

where  $N_q(T)$  represents the single-particle level density at the Fermi energy. At zero temperature it has the simple form

$$N_q = \frac{k_{Fq} E_{Fq}^*}{\pi^2}, \quad q = n, p.$$

In the symmetric case ( $F_0^{nn} = F_0^{pp}$ ,  $F_0^{np} = F_0^{pn}$ ), the Eqs. (27) and (28) correspond to the two Pomeranchuk instability conditions

$$\begin{aligned} F_0^s &= F_0^{nn} + F_0^{pp} < -1 && \text{(mechanical),} \\ F_0^a &= F_0^{nn} - F_0^{pp} < -1 && \text{(chemical).} \end{aligned} \quad (31)$$

From the dispersion relations  $F_0^s$  will give the properties of the density (isoscalar) modes while  $F_0^a$  is related to the concentration (isovector) modes. For asymmetric NM we have some corresponding generalized Landau parameters  $F_{0g}^s$  and  $F_{0g}^a$  which will characterize the collective response (respectively isoscalarlike and isovectorlike). They can be expressed as fixed combinations of the  $F_0^{q,q'}$  for each baryon density, asymmetry and temperature. This transformation is reducing Eq. (29) to a ‘‘diagonal’’ form [33]

$$\begin{aligned} (1 + F_{0g}^s)(1 + F_{0g}^a) &= \frac{4}{(1-y)\rho^2} \left( \frac{N_n N_p}{N_n + N_p} \right)^2 \\ &\times \left( \frac{\partial P}{\partial \rho} \right)_{T,y} \left( \frac{\partial \mu_p}{\partial y} \right)_{T,p}. \end{aligned} \quad (32)$$

As already discussed, in the unstable region of dilute asymmetric NM we have *isoscalarlike* unstable modes and so  $1 + F_{0g}^s < 0$ , while the combination  $1 + F_{0g}^a$  will stay positive. In Fig. 10 we report the full calculation of these two quantities in the unstable region at zero temperature, for

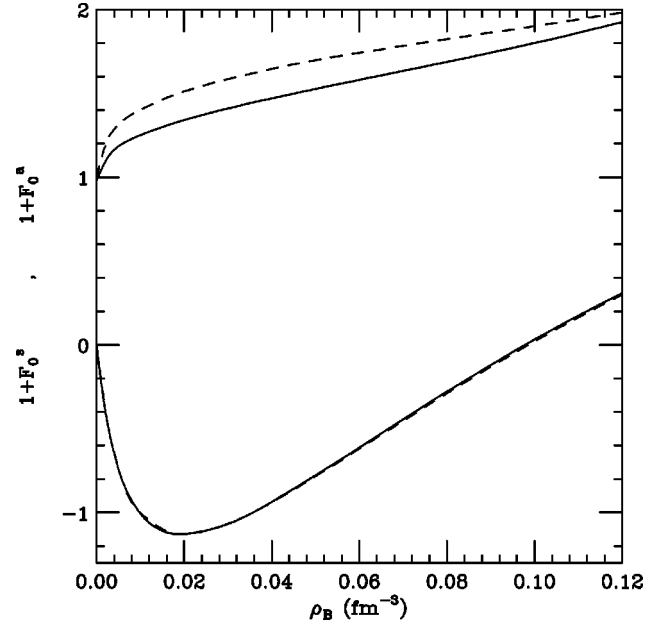


FIG. 10. Behavior of the generalized Landau parameters inside the instability region at zero temperature and asymmetry  $\alpha=0.5$  ( $N=3Z$ ). Dashed lines:  $(\rho)$ . Solid lines:  $(\rho + \delta)$ .

asymmetry  $\alpha=0.5$ , with and without the  $\delta$  coupling. The  $\delta$  meson almost does not affect the unstable mode given by the  $F_{0g}^s$  parameter. Hence the limits of the instability region, for  $\alpha=0.5$ , are not changed (see the Figs. 7–9). We have a much larger effect on the  $F_{0g}^a$  parameter which describes ‘‘stable’’ *isovectorlike* modes, that actually can propagate as good zero-sound collective motions since  $F_{0g}^a > 0$ . This can be expected from the isovector nature of the  $\delta$  meson. From this we obtain the main differences seen in Figs. 8 and 9 for the quantity [Eq. (26)] inside the instability region, just using Eq. (32).

Another interesting aspect of the comparison between Fig. 8 and Fig. 10 is the shift of the ‘‘maximum instability’’ density region. From the thermodynamical condition reported in Fig. 8, it seems that the largest instability (the most negative value) is around  $\rho_B = 0.06 \text{ fm}^{-3}$ . In fact, from Fig. 10 we see that the fastest unstable mode, corresponding to the most negative Pomeranchuk condition for  $1 + F_{0g}^s$ , is actually present for more dilute matter, around  $\rho_B = 0.02 \text{ fm}^{-3}$ . This shows the importance of the linear-response analysis. Finally, the fact that the  $\delta$  coupling mostly affects the *isovectorlike* modes is of great interest for possible effects on the isovector giant dipole resonances studied around normal density within the RMF approach in asymmetric systems.

## V. CONCLUSION AND OUTLOOK

The aim of this work has been to select interesting effects on properties of the asymmetric nuclear matter due to the coupling to the charged  $\delta$ -scalar meson. Simple analytical results allow one to clarify the interplay between the  $\rho$ - and  $\delta$ -meson contributions.

With respect to the equation of state, when  $\delta$  is included the symmetry energy retains an almost linear repulsive be-

havior at subnuclear densities, while it starts to move to a roughly parabolic trend above the saturation density  $\rho_0$ . Such an effect comes directly from the general relativistic property of the weakening of the attractive scalar interactions at high density. It represents an equivalent in the isovector channel (interplay of  $\rho$  and  $\delta$  contributions) to the saturation mechanism of the symmetric NM (the interplay of  $\omega$  and  $\sigma$  contributions). All this gives further fundamental support to the introduction of the  $\delta$  channel in the symmetry energy evaluation.

Such a “ $\delta$  mechanism” for the symmetry energy leads to a more repulsive EOS for pure neutron matter at baryon densities roughly above  $2\rho_0$ . This is the region where transitions to different forms of nuclear matter are expected, and so the result appears quite stimulating.

We have shown in detail that the  $\delta$  contributions are not negligible for the slope parameter around  $\rho_0$  (the *symmetry pressure*), and absolutely essential for the curvature parameter (*symmetry incompressibility*). The proton-neutron effective mass splitting is also directly given by the  $\delta$  coupling, and appears to be of the order of 15% at normal nuclear density (for  $N=3Z$  asymmetry).

The possibility of an experimental observation of such effects is suggested. Here we list some sensitive observables: (i) neutron distributions in  $n$ -rich nuclei (stable and unstable) [25–27]; (ii) assessment of drip-line stabilities [15,16]; (iii) bulk densities and incompressibility modulus in asymmetric nuclei [29,42,43]; and (iv) transport properties in radioactive beam collisions at intermediate energies: dissipative mechanisms, fast nucleon emission, and collective flows [18,28,34,36,44,56].

Effects on the critical properties of warm ANM, the mixing of mechanical and chemical instabilities and isospin distillation, are also presented. The border of the instability regions as well as the nature of the unstable fluctuations in dilute asymmetric matter are not much affected. Indeed, in the low-density region the symmetry energy has a very similar behavior with and without a  $\delta$  meson. This reduces the

possibility of the observation of  $\delta$ -coupling effects from measurements of isospin effects in multifragmentation events in asymmetric heavy-ion collisions. However, we note that other fragment production mechanisms, like *neck fragmentation*, are expected to be very sensitive to the symmetry potential around normal density since clusters are now formed in regions in contact with the “spectator” matter [35,36]. We can predict some interesting effects on this kind of event, that actually represent quite a large part of the fragment production cross section.

Moreover, from study of the  $\delta$  influence on the Landau parameters in the low baryon density region, we see an interesting effect on the collective response of asymmetric NM. While the unstable (*isoscalarlike*) modes are almost not modified, the *isovectorlike* ones, which have a good stable zero-sound propagation, are quite sensitive to the introduction of the  $\delta$ . This suggests some importance of the  $\delta$  meson in a RMF description of isovector giant resonances in asymmetric nuclei.

In conclusion, we would like to add a comment on the limits of the Hartree scheme used in this work, as well as in most RMF calculations. Indeed, it is well known that exchange terms can also give contributions in the isovector scalar channel in the absence of explicit  $\delta$  couplings, see Ref. [38], and references therein. The Dirac-Brueckner-Hartree-Fock results of Ref. [15], and some nonlinear-Hartree-Fock calculations performed in Ref. [38,57], show that an effective  $\delta$  coupling parameter  $f_\delta \approx 2.5 \text{ fm}^2$ , almost constant in a wide density range, is well accounting for the Fock term contributions. This makes us more confident in the reliability of the quantitative evaluation of the  $\delta$  effects discussed in this paper.

#### ACKNOWLEDGMENTS

One of the authors (L.B.) would like to thank the LNS in Catania for hospitality during his stay. This work was supported by the INFN of Italy and the National Natural Science Foundation of China.

- 
- [1] J.D. Walecka, *Ann. Phys. (N.Y.)* **83**, 491 (1974).  
 [2] B.D. Serot and J.D. Walecka, *Adv. Nucl. Phys.* **16**, 1 (1986); *Int. J. Mod. Phys. E* **6**, 515 (1997).  
 [3] Y. Sugahara and H. Toki, *Nucl. Phys.* **A579**, 557 (1994).  
 [4] G.A. Lalazissis, J. Konig, and P. Ring, *Phys. Rev. C* **55**, 540 (1997).  
 [5] M.M. Sharma, A.R. Farhan, and S. Mythili, *Phys. Rev. C* **61**, 054306 (2000).  
 [6] K. Sumiyashi and H. Toki, *Astrophys. J.* **422**, 700 (1994).  
 [7] C.H. Lee, *Phys. Rep.* **275**, 255 (1996).  
 [8] M. Prakash *et al.*, *Phys. Rep.* **280**, 1 (1997).  
 [9] I. Bombaci, in *Isospin Physics in Heavy Ion Collisions*, Ref. [18], pp. 35–81, and references therein.  
 [10] S. Yoshida, H. Sagawa, and N. Takigawa, *Phys. Rev. C* **58**, 2796 (1998).  
 [11] H. Mueller and B.D. Serot, *Phys. Rev. C* **52**, 2072 (1995).  
 [12] S. Kubis and M. Kutschera, *Phys. Lett. B* **399**, 191 (1997).  
 [13] H. Shen, Y. Sugahara, and H. Toki, *Phys. Rev. C* **55**, 1211 (1997).  
 [14] F. de Jong and H. Lenske, *Phys. Rev. C* **57**, 3099 (1998).  
 [15] F. Hofmann, C.M. Keil, and H. Lenske, *Phys. Rev. C* **64**, 034314 (2001).  
 [16] J. Leja and S. Gmuca, *Acta Phys. Slov.* **51**, 201 (2001); S. Gmuca, *Proceedings of the International Symposium on Exotic Nuclei, Baikal, 2001* (World Scientific, Singapore, in press).  
 [17] *Proceedings Nucleus-Nucleus Collisions VII* [*Nucl. Phys.* **A685**, 1 (2001)].  
 [18] *Isospin Physics in Heavy Ion Collisions*, edited by Bao-An Li and Udo Schroeder (Nova, Huntington, NY, 2001), pp. 1–480.  
 [19] J. Boguta and A.R. Bodmer, *Nucl. Phys.* **A292**, 413 (1977).  
 [20] A.R. Bodmer, *Nucl. Phys.* **A526**, 703 (1991).  
 [21] We would like to remark that, in general, nonlinear terms in the isoscalar vector channel  $\omega$  appear to be less important (see Refs. [11,22]), as also confirms the good nuclear structure re-

- sults of the  $NL3$  parametrization [4]. Also, in the case of the isovector vector channel  $\rho$ , nonlinear terms have been shown to have small effects [23].
- [22] R.J. Furnstahl and B.D. Serot, Nucl. Phys. **A671**, 447 (2000).
- [23] H. Mueller and B.D. Serot, Nucl. Phys. **A606**, 508 (1996).
- [24] C. J. Pethick and D. G. Ravenhall, Annu. Rev. Nucl. Part. Sci. **45**, 425 (1995).
- [25] B.A. Brown, Phys. Rev. Lett. **85**, 5296 (2000).
- [26] S. Typel and B.A. Brown, Phys. Rev. C **64**, 027302 (2001).
- [27] C.J. Horowitz and J. Piekarewicz, Phys. Rev. Lett. **86**, 5647 (2001).
- [28] M. Colonna, M. Di Toro, G. Fabbri, and S. Maccarone, Phys. Rev. C **57**, 1410 (1998).
- [29] M. Di Toro *et al.*, Prog. Part. Nucl. Phys. **42**, 125 (1999).
- [30] Bao-An Li and C.M. Ko, Nucl. Phys. **A618**, 498 (1997).
- [31] M. Colonna, M. Di Toro, and A. Larionov, Phys. Lett. B **428**, 1 (1998).
- [32] V. Baran, A. Larionov, M. Colonna, and M. Di Toro, Nucl. Phys. **A632**, 287 (1998).
- [33] V. Baran, M. Colonna, M. Di Toro, and V. Greco, Phys. Rev. Lett. **86**, 4492 (2001).
- [34] Bao-An Li, Phys. Rev. Lett. **85**, 4221 (2000).
- [35] M. Di Toro *et al.*, Nucl. Phys. **A681**, 426c (2001).
- [36] M. Di Toro *et al.*, Proceedings of the International Symposium on Exotic Nuclei, Baikal, 2001 (Ref. [16]); V. Baran *et al.*, nucl-th/0111065 [Nucl. Phys. A (to be published)].
- [37] This is the case of a RMF model in the Hartree approximation, mostly followed in all applications. For a discussion on the effects of the Fock terms see Ref. [38] and references therein.
- [38] V. Greco, M. Colonna, M. Di Toro, G. Fabbri, and F. Matera, Phys. Rev. C **63**, 035202 (2001); **64**, 045203 (2001).
- [39] This choice corresponds to the  $\delta$  parameters ( $g_{\delta}, m_{\delta}$ ) of the *BonnC* potential [40]. We note that such a value is also in quite good agreement with the density-dependent study of Ref. [15], derived from a microscopic Dirac-Brueckner-Hartree-Fock calculation in a asymmetric matter (the plateau in Fig. 2 of that reference). In any case we are interested in the qualitative features of the  $\delta$  coupling.
- [40] R. Machleidt, Adv. Nucl. Phys. **19**, 189 (1989).
- [41] S. Fantoni, A. Sarsa, and K.E. Schmidt, Phys. Rev. Lett. **87**, 181101 (2001).
- [42] M. Lopez-Quelle, S. Marcos, R. Niembro, A. Bouyssy, and N. Van Giai, Nucl. Phys. **A483**, 479 (1988).
- [43] Bao-An Li, Nucl. Phys. **A681**, 434c (2001).
- [44] Bao-An Li, C.M. Ko, and W. Bauer, Int. J. Mod. Phys. E **7**, 147 (1998).
- [45] We note that in the nonrelativistic case the kinetic contribution to  $K_{sym}$  is actually negative, since it has the form  $-\pi^2\rho_0/(Mk_F)$  which is of the order  $\sim -30$  MeV. In the relativistic case it becomes slightly positive due to the density dependence of the nucleon effective mass.
- [46] The solid lines in Fig. 4 are not fully symmetric with respect to the  $\alpha=0$  dashed line. This is due to the fact that, for a fixed baryon density, the total scalar density which gives the  $\sigma$  field contribution [first part of Eq. (6)], is also slightly  $N/Z$  dependent.
- [47] W. Zuo, I. Bombaci, and U. Lombardo, Phys. Rev. C **60**, 024605 (1999).
- [48] E. Chabanat, P. Bonche, P. Haensel, J. Meyer, and R. Schaefer, Nucl. Phys. **A627**, 710 (1997).
- [49] H. Huber, F. Weber, and M.K. Weigel, Phys. Rev. C **57**, 3484 (1997).
- [50] G. Sauer, H. Chandra, and U. Mosel, Nucl. Phys. **A264**, 221 (1976).
- [51] G.F. Bertsch and P.J. Siemens, Phys. Lett. **126B**, 9 (1983).
- [52] H.R. Jaqaman, A.Z. Mekjian, and L. Zamick, Phys. Rev. C **29**, 2067 (1984).
- [53] Of course we can have other asymmetric NM instability regions, at higher baryon densities, with a different structure of the unstable modes [33]. Here some interactions even predict quite exciting *isovectorlike* (species separation) unstable oscillations. Unfortunately all this is not included in the present experimental possibilities.
- [54] L. D. Landau and E. M. Lifshitz, *Statistical Physics* (Pergamon, Oxford, 1980), p. 208.
- [55] G. Baym and C. Pethick, *Landau Fermi-Liquid Theory* (Wiley, New York, 1991).
- [56] L. Scalone, M. Colonna, and M. Di Toro, Phys. Lett. B **461**, 9 (1999).
- [57] V. Greco, Ph.D. thesis, University of Catania, 2001.